Feasibility of simultaneous ^{99m}Tc-tetrofosmin and ^{123}I-BMIPP dual-tracer imaging with cadmium-zinc-telluride detectors in patients undergoing primary coronary intervention for acute myocardial infarction

Yoshihiro Yamada, MD,[a] Shintaro Nakano, MD, PhD,[a] Youdou Gatate, MD,[a] Nanami Okano, MD, PhD,[b] Toshihiro Muramatsu, MD, PhD,[a] Shigeyuki Nishimura, MD, PhD,[a] Ichiei Kuji, MD, PhD,[c] Kenji Fukushima, MD, PhD,[c] and Ichiro Matsunari, MD, PhD[b]

[a] Department of Cardiology International Medical Center, Saitama Medical University, Saitama, Japan
[b] Division of Nuclear Medicine, Department of Radiology, Saitama Medical University, Saitama, Japan
[c] Department of Nuclear Medicine International Medical Center, Saitama Medical University, Saitama, Japan

Received Oct 22, 2018; accepted Dec 17, 2018
doi:10.1007/s12350-018-01585-9

Background. **Simultaneous dual-tracer imaging using isotopes with close photo-peaks may benefit from improved properties of cadmium-zinc-telluride (CZT)-based scanners.**

Methods. **Thirty patients having undergone primary percutaneous coronary intervention for acute myocardial infarction underwent single-(^{99m}Tc-tetrofosmin (TF) or ^{123}I-BMIPP first) followed by simultaneous ^{99m}Tc-TF /^{123}I-BMIPP dual-tracer imaging using a Discovery NM/CT 670 CZT. The values for the quantitative gated-SPECT (QGS) and the quantitative perfusion SPECT (QPS) were assessed.**

Results. **The intra-class correlation (ICC) coefficients between the single- and dual-tracer imaging were high in all the QGS and QPS data (Summed motion score: 0.95, summed thickening score: 0.94, ejection fraction: 0.98, SRS for ^{99m}Tc-TF: 0.97/ for ^{123}I-BMIPP: 0.95). Wall motion, wall thickening and rest scores per coronary-territory-based regions were also comparable between the single- and dual imaging (ICC coefficient > 0.91). The interrater concordance in the visual analysis for the infarction and perfusion-metabolism mismatch was significant for the global and regional left ventricle ($P < 0.001$).**

Conclusion. **The quantitative/semi-quantitative values for global and regional left-ventricular function, perfusion, and fatty acid metabolism were closely comparable between the dual-tracer imaging and the single-tracer mode. These data suggests the feasibility of the novel CZT-based scanner for the simultaneous ^{99m}Tc-TF /^{123}I-BMIPP dual-tracer acquisitions in clinical settings. (J Nucl Cardiol 2021;28:187–95.)**

Key Words: Perfusion-metabolism mismatch • CZT camera • acute myocardial infarction • dual imaging

Electronic supplementary material The online version of this article (https://doi.org/10.1007/s12350-018-01585-9) contains supplementary material, which is available to authorized users.

The authors of this article have provided a PowerPoint file, available for download at SpringerLink, which summarizes the contents of the paper and is free for re-use at meetings and presentations. Search for the article DOI on SpringerLink.com.

Reprint requests: Shintaro Nakano, MD, PhD, Department of Cardiology, International Medical Center, Saitama Medical University 1397-1 Yamane, Hidaka, Saitama 350-1298, Japan; *snakano@saitama-med.ac.jp*

1071-3581/$34.00

See related editorial, pp. 196–198

INTRODUCTION

Free fatty acid is a main myocardial energy source under normal conditions, but under ischemic conditions, myocardial metabolism preferentially shifts from aerobic β oxidization of free fatty acid in mitochondria to anaerobic glycolysis in cytosol.[1,2] Under a condition called post-ischemic metabolic stunning, reduced uptake of ^{123}I-β-methyl-*p*-iodophenlypentadecanoic acid (BMIPP), which reflects impaired myocardial β oxidization is prolonged despite restoration of perfusion.[3,4] Such a perfusion-metabolism mismatch, where the deficit of free fatty acid metabolism is discordantly more severe than that of perfusion, is known to be predictive of myocardial viability and prognosis in chronic ischemia[5,6] and in the (sub)acute phase of myocardial infarction,[7,8] and can be evaluated by dual-isotope nuclear imaging. ^{99m}Tc-labelled isotopes ($t_{1/2}$= 6 hours) are theoretically preferable perfusion radiotracers to ^{201}Tl-based ones ($t_{1/2}$ = 73 hours), as they have a shorter physical half time and higher photon-energy, leading to less attenuation artifact and radiation exposure.[9] However, as the photopeaks of ^{99m}Tc (140 keV) and ^{123}I (159 keV) are close, quantitative assessment using simultaneous acquisition of ^{99m}Tc-/^{123}I-labelled dual tracers is challenging.[10,11] Recently, semiconductor cadmium-zinc-telluride (CZT) detectors have been launched in clinical settings, and they have provided shorter scanning times while improving energy and spatial resolution in comparison with conventional NaI scintillation detectors.[10,12-15] More recently, a novel SPECT scanner with CZT detectors, the Discovery NM/CT 670 CZT (GE Healthcare, Milwaukee, Wisconsin), was developed for whole-body imaging including cardiac SPECT imaging. This novel scanner is equipped with 130 pixelated detectors with registered collimation to improve the overall system resolution, as well as the energy resolution; although evidence of the benefits of these features from clinical settings is currently lacking, these are promising properties for multi-tracer imaging.

In our current study, we sought to evaluate the utility of a Discovery NM/CT 670 CZT for simultaneous ^{99m}Tc-tetrofosmin (TF)/^{123}I-BMIPP dual-isotope acquisitions by comparing dual-tracer imaging with single-tracer imaging, in patients having undergone primary percutaneous coronary intervention (PCI) for acute myocardial infarction (AMI).

METHODS

Study Design and Patient Selection

Patients aged over 20 years who underwent PCI for AMI from December 2017 to June 2018 at Saitama Medical University, International Medical Center, were prospectively recruited for this study (UMIN ID: 00029768). Patients with an artificial pacemaker, potential pregnancy, potential inability to complete the examination due to mental or physical reasons, or recent myocardial perfusion/metabolism imaging, were excluded. This study was approved by the Institutional Review Board of Saitama International Medical Center (reference number: 17-126) and Saitama Medical University (reference number: 17-094). All patients signed written informed consent.

Clinical Data Collection

Baseline demographics, electrocardiographic findings, and data regarding disease severity and in-hospital course were recorded.

Examination Protocol

After completion of in-hospital cardiac rehabilitation, patients underwent a 1-day ^{99m}Tc-TF (Nihon Medi-physics Co., Ltd., Tokyo, Japan) and ^{123}I-BMIPP (Nihon Medi-Physics Co., Ltd.) dual-isotope imaging examination at Saitama Medical University Hospital. All examinations were performed under electrocardiographic gating, as recommended for quantification.[16] Patients were assigned to either a ^{99m}Tc-TF or ^{123}I-BMIPP first protocol (Figure 1). In the ^{99m}Tc-TF first protocol, single-tracer ^{99m}Tc-TF gated-SPECT/CT imaging was first acquired followed by a dual-tracer gated-SPECT/CT acquisition. In the ^{123}I-BMIPP first protocol, single-tracer ^{123}I-BMIPP gated-SPECT/CT was first acquired followed by a dual-tracer gated-SPECT/CT acquisition.

SPECT Data Acquisition and Post-processing of Images

The Discovery NM/CT 670 CZT has 130 CZT modules and wide-energy high-resolution collimators. Each detector contained 32 × 32 pixelated 2.46 × 2.46 mm CZT elements. Using the Lister tool (GE Healthcare) on a Xeleris 4.0 workstation (GE Healthcare), images with 30 views/scan and 65 seconds/view were reframed. The peak energy and window widths were set to 140 ± 7.5% and 159 ± 7.5% KeV for ^{99m}Tc-TF and ^{123}I-BMIPP, respectively, as recommended by GE Healthcare. Using the Myocardial Evolution software for ^{99m}Tc and ^{123}I (GE Healthcare) supplied on the same workstation, images for quantitative gated-SPECT (QGS) and quantitative perfusion SPECT (QPS) were reconstructed to obtain views in the standard axes (short axis, vertical long axis and horizontal axis) and polar maps of the left ventricle. The iterative algorithm with integrated collimator geometry modeling used maximum penalized likelihood iterative reconstruction.[17] A Butterworth post-processing filter (critical frequency, 0.4 cycle/cm; order, 10) was applied to the reconstructed slices.[17] Attenuation correction was not applied because it would have resulted in low uniformity.[10] Manual processing was applied as necessary to adjust the left-ventricular axis, center, and endocardial/epicardial contour with masking/constraint of extracardiac accumulation.

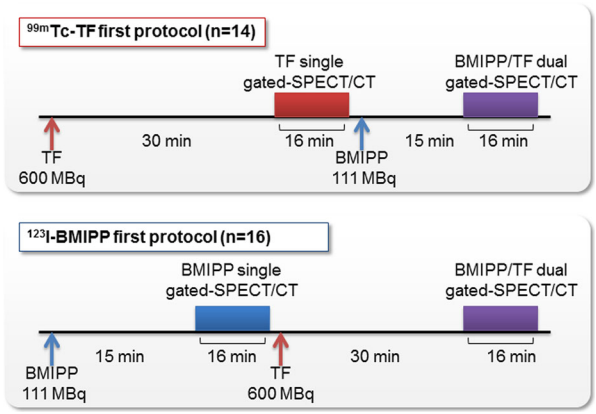

Figure 1. Schema of the examination protocols. Patients were assigned to either a ^{99m}Tc-TF or ^{123}I-BMIPP first protocol. All acquisition times were set for 16 minutes. ^{99m}Tc-TF and ^{123}I-BMIPP were injected 30 and 15 minutes prior to initiation of acquisition, respectively. The injected isotope doses were fixed at 600 and 111 MBq for ^{99m}Tc-TF and ^{123}I-BMIPP, respectively.

Image Analysis

The left-ventricular myocardium was divided in to 17 segments,[18] and the vascular territories corresponding to the three major coronary arteries were defined, with the anterior, septal and apical regions being assigned to the left anterior descending artery (LAD), the inferior region to the right coronary artery (RCA), and the lateral region to the left circumflex artery (LCX).[18] For the QGS with ^{99m}Tc-TF, the following parameters were assessed. Left-ventricular wall motion (mm) and wall thickening (%) in each segment, and the summed values per coronary territory were recorded. Semi-quantitative scales for the wall motion and the wall thickening were automatically assigned to each segment to calculate the summed motion scores (SMS) and summed thickening scores (STS) of all segments.[19] Left-ventricular end-diastolic volume (EDV, ml), end-systolic volume (ESV, ml), and ejection fraction (EF, %) were recorded. For the QPS with ^{99m}Tc-TF and ^{123}I-BMIPP, the following parameters were assessed. Semi-quantitative scales for uptake of radioactive counts was automatically assigned to each segment to calculate the summed rest scores (SRS) of all segments, and the summed values per coronary territory were recorded.[20] The mismatch scores were then calculated as SRS for BMIPP-TF. The perfusion extent (%) and the total perfusion deficit (TPD, %) were recorded. A summary and details of the quantitative and semi-quantitative analysis are shown in Supplementary Table 1 and Figure 1.

For the visual analysis, two experienced nuclear radiologists (I.M. and K.F.) interpreted the dual-tracer imaging for the presence or absence of infarction and perfusion-metabolism mismatch (stunning/hibernation) in the global left ventricle (i.e., per patient basis), and the LAD, RCA and LCX coronary territories.

Statistical Analysis

Continuous variables are expressed as the mean ± standard deviation or median [first-third quartile], and categorical variables as number (%). The Shapiro–Wilk test was performed to test for normal distributions.

The correlation between the quantitative values obtained from dual- and single-tracer imaging was evaluated using intra-class correlation (ICC; two-way mixed-effects model, for consistency) and Bland–Altman analysis. Repeatability and reproducibility of the quantitative analysis with respect to intra-(S.N.) and inter-(S.N. and I.M) observer variability were evaluated using ICC (two-way mixed-effects model for absolute agreement) and ICC (two-way random-effects model, for absolute agreement), respectively, with the reframed dual-tracer images of ten patients being randomly assigned to each analysis.

The concordance in the visual analysis was evaluated using unweighted κ statistics between the interpretations of the two radiologists.

Statistical analyses were performed using JMP Pro 11.2.0 (SAS Institute Inc., Cary, NC, USA) or SPSS statistics software (version 25, IBM Corp., Armonk, NY, USA), as appropriate.

RESULTS

Clinical Characteristics of the Studied Patients

From December 2017 to June 2018, 110 consecutive patients who underwent primary PCI for AMI at Saitama Medical University, International Medical Center, were screened. After application of the exclusion criteria, 31 patients participated in the study, with one patient being further excluded from the final analysis because of a suspected CD36 deficiency (Supplementary Figure 2). The characteristics of the remaining 30 patients (^{99m}Tc-TF first protocol: n = 14, ^{123}I-BMIPP first protocol: n = 16) are shown in Table 1.

Concordance in the Visual Analysis of Dual-Tracer Imaging

The Cohen's κ coefficients between the two radiologists for the presence of infarction and perfusion-metabolism mismatch were 0.85 ($P < 0.001$) and 1.00 ($P < 0.001$), respectively for the global left ventricle, and 0.94 ($P < 0.001$) and 0.89 ($P < 0.001$) for the coronary territory-based regions of the left ventricle (a total of 90 territories).

Quantification and Semi-quantification of Dual- and Single-Tracer Imaging

The ICC coefficient with 95% confidence interval and the Bland–Altman mean of difference with 95%

limits of agreement between the values obtained from dual- and single-tracer imaging are shown in Figures 2, 3, and 4. The ICC coefficients between dual- and single-tracer imaging were high (> 0.91) in all the data. The correlations were high in the QGS for the global left ventricle (Figure 2), except for apparent outlying EDV (Figure 2C) and ESV (Figure 2D) values in a patient with a severely dilated left ventricle and prominent extra-cardiac accumulation. No obvious tracer-specific trend was observed in the QPS results from the global left ventricle (Figure 3), and no obvious coronary territory-related heterogeneity was observed in the QGS and QPS regional left ventricle data (Figures 4, 5; Supplementary Figure 3).

Repeatability and Reproducibility

The ICC coefficients for the repeatability and reproducibility analysis were high (> 0.93) in all the data; the intra- and inter-observer ICC coefficients were 1.00 and 0.99 for SMS, 1.00 and 0.99 for STS, 1.00 and 1.00 for EF, 0.98 and 1.00 for SRS on ^{99m}Tc-TF, and 0.99 and 0.98 for SRS on ^{123}I-BMIPP. The details are shown in Supplementary Table 2.

DISCUSSION

Main Findings

Our current study first demonstrated that a Discovery NM/CT 670 CZT scanner could be used for simultaneous ^{99m}Tc-TF /^{123}I-BMIPP dual-tracer acquisitions, affording clinically available and reproducible images in patients with AMI having undergone primary PCI. The quantitative and semi-quantitative values for global and regional left-ventricular function, perfusion, and fatty acid metabolism obtained from the simultaneous ^{99m}Tc-TF /^{123}I-BMIPP dual-tracer isotope acquisitions were closely comparable to those obtained

Table 1. Patient characteristics

Total *n* = 30 (^{99m}Tc-TF first *n* = 14, ^{123}I-BMIPP first *n* = 16)	
Demographics and concomitant conditions	
Age, years	61.5 ± 10.8
Man, *n* (%)	25 (83.3%)
Body mass index, kg/m^2	24.2 ± 4.1
Body surface area, m^2	1.77 [1.64–1.82]
Hypertension, *n* (%)	15 (50.0%)
Diabetes mellitus, *n* (%)	9 (30.0%)
Dyslipidemia, *n* (%)	15 (500%)
End-stage renal disease, *n* (%)	1 (0.3%)
Current smoking, *n* (%)	8 (26.7%)
Previous myocardial infarction, *n* (%)	1 (0.3%)
Electrocardiographic findings	
Atrial fibrillation rhythm, *n* (%)	0 (0.0%)
ST-T segment elevation, *n* (%)	29 (96.7%)
Severity and clinical course	
Time from onset to reperfusion, hours	4.0 [3.0–5.0]
Killip class ≥ III, *n* (%)	3 (10.0%)
Maximum serum creatinine kinase, IU/L	1597 [897–4691]
Maximum serum creatinine kinase MB isozyme, ng/mL	173 [72–345]
Culprit coronary artery, *n* (%)	
Left main trunk–anterior descending artery	17 (56.7%)
Right coronary artery	9 (30.0%)
Left circumflex artery	4 (13.3%)
Multivessel disease, *n* (%)	18 (60.0%)
In-hospital death, *n* (%)	0 (0.0%)

Data are presented as mean ± standard deviation for continuous variables or median [1st–3rd quartile] and as number (percentage) for categorical variables

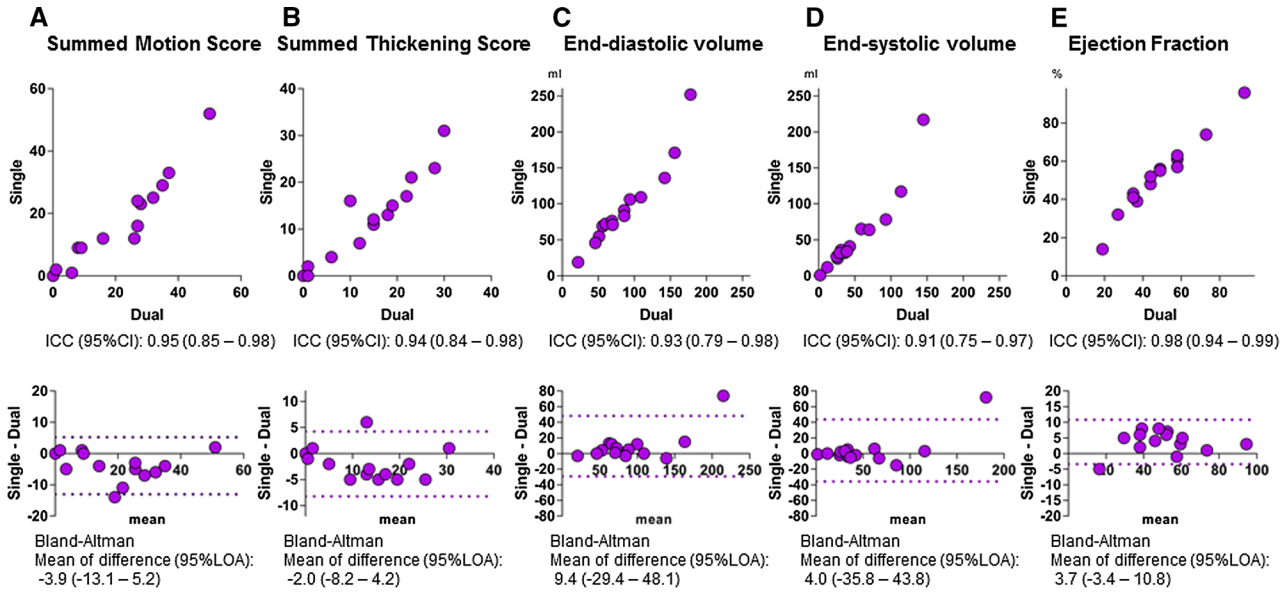

Figure 2. Quantitative Gated SPECT (QGS) for the global left ventricle: dual- vs single-tracer imaging. Upper graphs: Intra-class correlation (ICC) between the QGS data for the global left ventricle obtained from dual- (*x* axis) and single- (*y* axis) tracer imaging. Lower graphs: Bland-Altman analysis showing mean (x axis) and difference between (*y* axis) the corresponding two values. *CI*, confidence interval; *LOA,* limit of agreement.

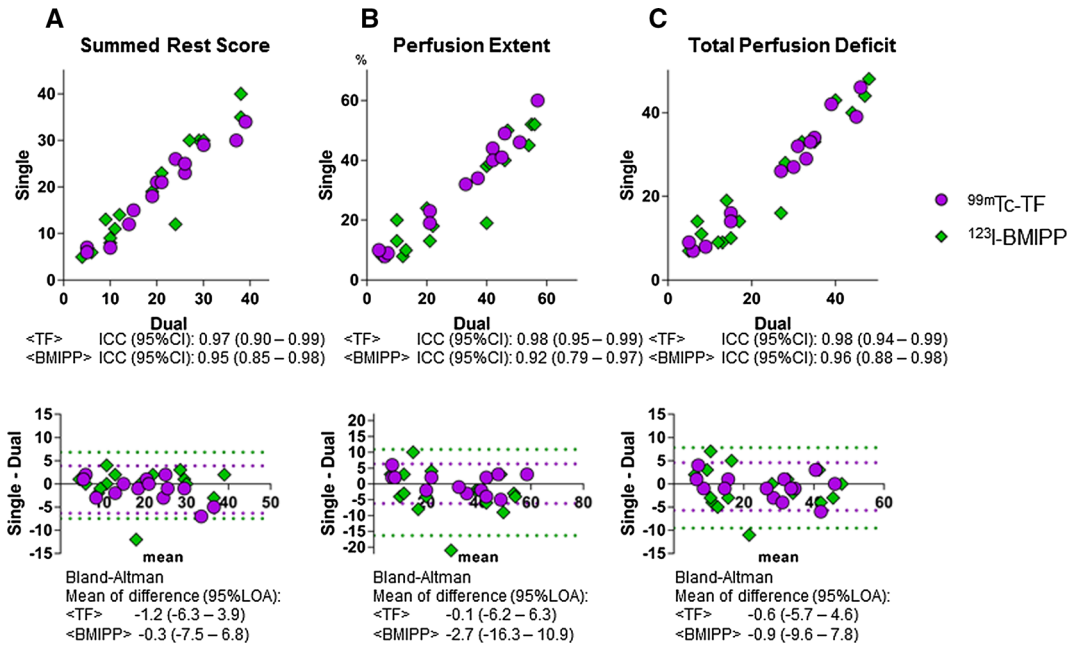

Figure 3. Quantitative Perfusion SPECT (QPS) for the global left ventricle: dual- vs single-tracer imaging. Upper graphs: Intra-class correlation (ICC) between dual- and single-tracer QPS data for the global left ventricle, Lower graphs: Bland-Altman analysis. *CI*, confidence interval; *LOA*, limit of agreement. Purple circle: ^{99m}Tc-TF, Green diamond: ^{123}I-BMIPP.

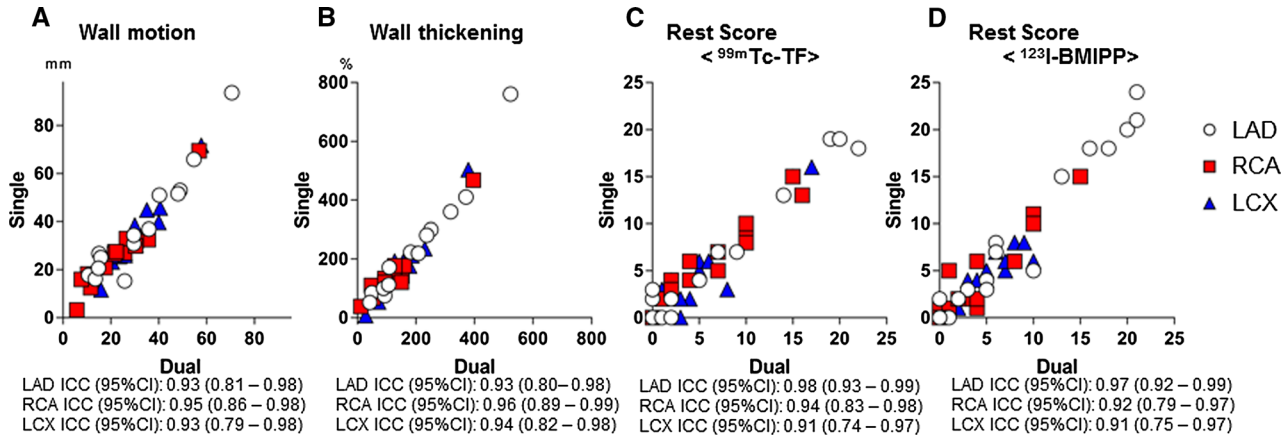

Figure 4. Quantitative Gated/Perfusion SPECT (QGS/QPS) per coronary territory: dual- vs single-tracer imaging. Upper graphs: Intra-class correlations (ICC) between dual- and single-tracer QGS/QPS data per coronary territory. *CI*, confidence interval; *LOA*, limit of agreement. White circle: Left anterior descending artery, red square: right coronary artery, blue triangle: left circumflex.

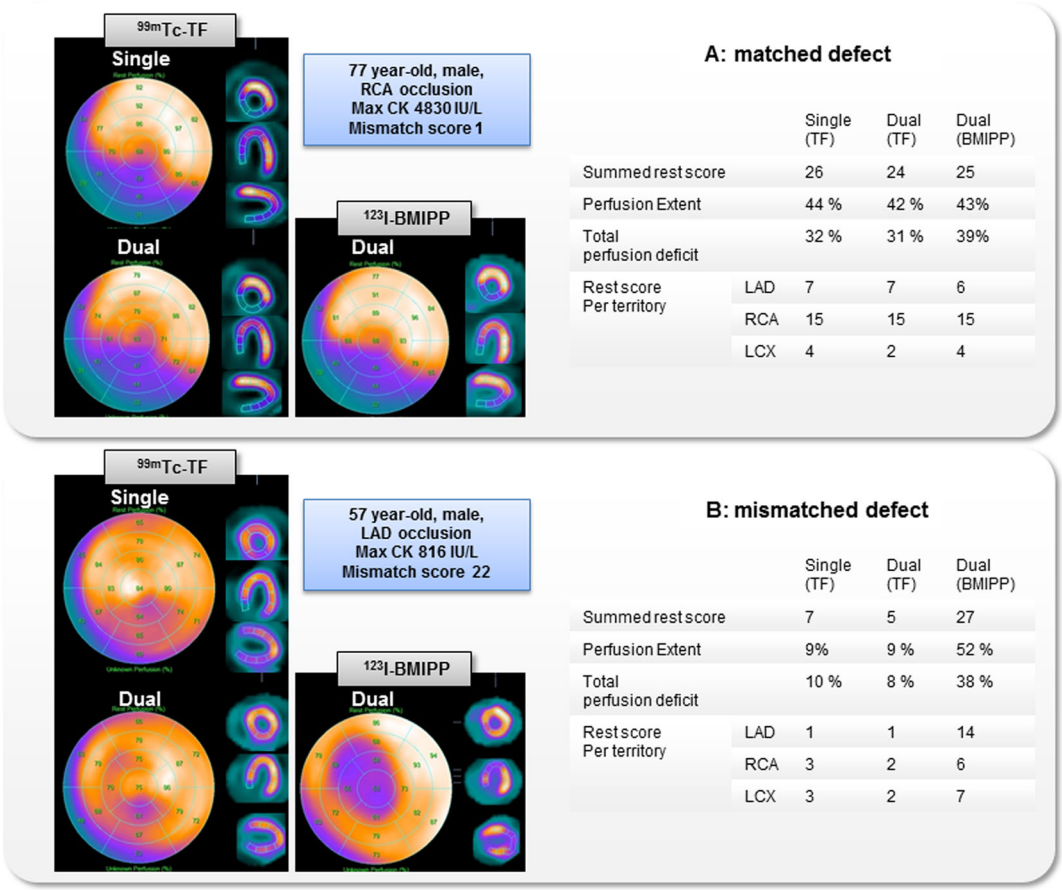

Figure 5. Representation of dual- and single-tracer Quantitative Perfusion SPECT (QPS) imaging. Quantitative Perfusion SPECT images for ^{99m}Tc-TF obtained from single-(^{99m}Tc-TF alone) and dual-(^{99m}Tc-TF and ^{123}I-BMIPP) tracer. (**A**) a 77-year-old man with right coronary artery occlusion showing a matched defect pattern (mismatch score: 1). (**B**) a 57-year-old man with left anterior descending artery occlusion showing a mismatched defect pattern (mismatch score: 22).

in the single-tracer mode, possibly owing to the properties of the novel scanner.

Utility of CZT Detectors for Myocardial Perfusion and Cardiac Function in Coronary Artery Disease

Currently, there are two semiconductor CZT camera systems available commercially, the Discovery NM/CT series (530c and 670 CZT) and the D-SPECT (Spectrum Dynamics, Biosensors, Caesarea, Israel). Although the collimation and reconstruction algorithms are different, the heart-centric techniques of the Discovery NM/CT 530c and D-SPECT, and the specific reconstruction algorithms facilitate enhanced count sensitivity, improved energy, and higher spatial resolution than conventional NaI crystal detectors.[13,21-24] Consequently, the advent of these CZT detectors has led to improved image quality, and a reduction in acquisition time and/or radiation exposure.[17,25,26]

In patients with known or suspected coronary artery disease, fast myocardial perfusion imaging using CZT-based detectors has provided better diagnostic accuracy with improved regional sensitivity compared with conventional cameras.[27,28] Left-ventricular global and regional functions have also been assessed using CZT-based scanners, with quantification of EF and the regional extent of scarring being similar to measurements made on magnetic resonance imaging,[29] and the EF demonstrating higher reproducibility than achieved with a conventional NaI camera.[30] Our study demonstrated that the quantitative and semi-quantitative parameters obtained for myocardial perfusion and cardiac function were highly reproducible, both for global left ventricle and regional measures (Supplementary Table 1).

Simultaneous ^{99m}Tc-TF /^{123}I-BMIPP Dual-Isotope Acquisition Using CZT Detectors

Areas showing a perfusion-metabolism mismatch may correspond to jeopardized but viable myocardium as functional improvement in such areas has been observed after revascularization.[7,8,31-33] ^{123}I-BMIPP is a commonly used tracer for evaluation of myocardial-free fatty acid metabolism in clinical studies.[3,5-8,34] On the other hand, for myocardial perfusion, ^{201}Tl, which has been recognized as providing a diagnostic accuracy similar to the ^{99m}Tc-family of tracers in most coronary artery disease[35], may frequently be used in simultaneous dual-isotope imaging in combination with ^{123}I-BMIPP, as the distant photo peaks of the two tracers facilitate enhanced energy resolution.[36,37] ^{99m}Tc-TF may be a theoretically preferable perfusion tracer in respect to better image quality, as it has a shorter half time and administration of higher dose is possible. However, when used in combination, the close photo-peaks of the ^{99m}Tc- and ^{123}I-isotopes require a special attention to discriminate their energy properties while maintaining count sensitivity. To ameliorate potentially interfering factors in dual-tracer imaging using conventional NaI scanners such as scatter contamination of isotopes, cross-talk from the primary photons of each radionuclide, attenuation and distance-dependent collimator responses, techniques using constrained spectral factor analysis, artificial neural networks and Monte Carlo-based joint ordered-subset expectation maximization iterative reconstruction have been applied, although all required complicated data processing[22,38,39]. Instead, using CZT scanners, excellent concordance between ^{99m}Tc-/^{123}I-labeled dual- and single-images has been demonstrated in both phantom and animal studies,[10,40] with the excellent spatial and energy resolution of the CZT scanners allowing the count sensitivity to be maintained. A previous phantom study using similar CZT-scanner systems showed improved energy resolution for dual-tracer imaging (300 MBq of ^{99m}Tc-TF and 100 MBq of ^{123}I-BMIPP), with only 4.0% downscatter contamination from ^{123}I-BMIPP in the energy window of ^{99m}Tc-TF and almost no upscatter contamination from ^{99m}Tc-TF in that of ^{123}I-BMIPP.[10] A clinical study on simultaneous ^{99m}Tc-MIBI/^{123}I-BMIPP dual-tracer imaging using the D-SPECT system showed the correct detection (in comparison with angiographic findings) of infarcted and stunned areas in patients who underwent revascularization for AMI.[11] In our current clinical study, we demonstrated images, and quantitative and semi-quantitative values obtained from ^{99m}Tc-/^{123}I-labeled dual-tracer imaging on a Discovery NM/CT 670 CZT that were analogous to those obtained from single-tracer imaging with fixed window settings in most of the studied patients. Exceptionally, one patient with a severely dilated left ventricle with low LVEF (LVEDV/LVESV = 178/145 ml, LVEF 19% in dual-mode) revealed a prominent discrepancy between the single- and dual-tracer data. In this patient, enhanced extra-cardiac accumulation and weak cardiac uptake might have led to inaccurate QGS analysis. Furthermore, another outlier that revealed discrepant results in the QPS for BMIPP demonstrated a failure in the automatic and manual QPS processing to adjust the endocardial/epicardial contour. The Discovery NM/CT 670 CZT has each collimator registered with a single semi-conductor detector pixel, which affords high resolution (6.4 mm at center) and image contrast. Together with the thick detector (7.5 mm in thickness) designed for improved count sensitivity, these properties of the scanner are beneficial for multi-tracer imaging. Our current study

demonstrated remarkable interrater agreement in visual interpretation of infarction and perfusion-metabolism mismatch in the global and regional left ventricle, suggesting promising clinical feasibility of the Discovery NM/CT 670 CZT for simultaneous ^{99m}Tc-TF /^{123}I-BMIPP dual-tracer imaging. The coronary territories defined by the radiologists were also compatible with angiographic findings. Disagreement on the infarcted area was observed in patients with modest infarction (n = 2), and on the perfusion-metabolism mismatched area in patients with mildly impaired free fatty acid metabolism (n = 1) and concomitant hibernation (n = 1). The patients with a visually determined mismatched defect (n = 17) tended to show a higher mismatch score (SRS for BMIPP-TF) than those without such a defect (n = 13) (6 [2-12]) vs 2 [2-4], P = 0.095, Supplementary Figure 4).

LIMITATIONS

This study has some limitations. First, it is a single-center, observational study with a relatively small number of patients. Using R version 3.5.1, package ICC.Sample.Size, the p0 (ICC coefficient for null hypothesis) was 0.60 to achieve a power of 0.80, when p (ICC coefficient obtained in the study) = 0.90, α = 0.05, and N = 14. However, we suggest that the correlation between the values obtained from dual- and single-tracer imaging, as well as intra- and inter-observer variability, are sufficient to propose the clinical feasibility of the technique. Further confirmative studies on larger numbers of patients are needed to ensure that our findings apply to heterogenous clinical cases, particularly those showing low LVEF. Second, the time elapsed from AMI onset to examination varied, with a median value of 25 days.[16-26] Therefore, post-ischemic functional recovery owing to revascularization may not have been appropriately predicted, as metabolic alterations may have been resolved in some patients with delayed examination.[41]

NEW KNOWLEDGE GAINED

We demonstrated the clinical feasibility of the Discovery NM/CT 670 CZT with a novel CZT detector for simultaneous ^{99m}Tc-TF /^{123}I-BMIPP dual-tracer isotope acquisitions in patients with AMI having undergone primary PCI. The quantitative and semi-quantitative values obtained from the dual-tracer mode for global and regional left-ventricular function, perfusion, and fatty acid metabolism were closely comparable to those obtained in the single-tracer mode, possibly owing to the improved energy and spatial resolution as well as count sensitivity of the new scanner.

Acknowledgements

The authors acknowledged to technical staffs in the Saitama Medical University Hospital and Mr. Hideyasu Hosono (GE Healthcare) for their technical support in performing imaging examination and analysis.

Disclosure

None.

References

1. Stanley WC, Lopaschuk GD, Hall JL, McCormack JG. Regulation of myocardial carbohydrate metabolism under normal and ischaemic conditions. Potential for pharmacological interventions. Cardiovasc Res 1997;33:243-57.
2. Bolli R. Myocardial 'stunning' in man. Circulation 1992;86:1671-91.
3. Dilsizian V, Bateman TM, Bergmann SR, Des Prez R, Magram MY, Goodbody AE, et al. Metabolic imaging with beta-methyl-*p*-[(123)I]-iodophenyl-pentadecanoic acid identifies ischemic memory after demand ischemia. Circulation 2005;112:2169-74.
4. Bergmann SR. Imaging of myocardial fatty acid metabolism with PET. J Nucl Cardiol 2007;14:S118-24.
5. Dobbeleir AA, Hambye AS, Franken PR. Influence of methodology on the presence and extent of mismatching between 99 mTc-MIBI and 123I-BMIPP in myocardial viability studies. J Nucl Med 1999;40:707-14.
6. Tamaki N, Tadamura E, Kawamoto M, Magata Y, Yonekura Y, Fujibayashi Y, et al. Decreased uptake of iodinated branched fatty acid analog indicates metabolic alterations in ischemic myocardium. J Nucl Med 1995;36:1974-80.
7. Hambye AS, Vervaet A, Dobbeleir A, Dendale P, Franken P. Prediction of functional outcome by quantification of sestamibi and BMIPP after acute myocardial infarction. Eur J Nucl Med 2000;27:1494-500.
8. Franken PR, Dendale P, De Geeter F, Demoor D, Bossuyt A, Block P. Prediction of functional outcome after myocardial infarction using BMIPP and sestamibi scintigraphy. J Nucl Med 1996;37:718-22.
9. Sogbein OO, Pelletier-Galarneau M, Schindler TH, Wei L, Wells RG, Ruddy TD. New SPECT and PET radiopharmaceuticals for imaging cardiovascular disease. Biomed Res Int 2014;2014:942960.
10. Kobayashi M, Matsunari I, Nishi K, Mizutani A, Miyazaki Y, Ogai K, et al. Simultaneous acquisition of (99 m)Tc- and (123)I-labeled radiotracers using a preclinical SPECT scanner with CZT detectors. Ann Nucl Med 2016;30:263-71.
11. Ko T, Utanohara Y, Suzuki Y, Kurihara M, Iguchi N, Umemura J, et al. A preliminary feasibility study of simultaneous dual-isotope imaging with a solid-state dedicated cardiac camera for evaluating myocardial perfusion and fatty acid metabolism. Heart Vessel 2016;31:38-45.
12. Madsen MT. Recent advances in SPECT imaging. J Nucl Med 2007;48:661-73.
13. Gambhir SS, Berman DS, Ziffer J, Nagler M, Sandler M, Patton J, et al. A novel high-sensitivity rapid-acquisition single-photon cardiac imaging camera. J Nucl Med 2009;50:635-43.
14. Bocher M, Blevis IM, Tsukerman L, Shrem Y, Kovalski G, Volokh L. A fast cardiac gamma camera with dynamic SPECT capabilities: Design, system validation and future potential. Eur J Nucl Med Mol Imaging 2010;37:1887-902.

15. Chowdhury FU, Vaidyanathan S, Bould M, Marsh J, Trickett C, Dodds K, et al. Rapid-acquisition myocardial perfusion scintigraphy (MPS) on a novel gamma camera using multipinhole collimation and miniaturized cadmium-zinc-telluride (CZT) detectors: Prognostic value and diagnostic accuracy in a 'real-world' nuclear cardiology service. Eur Heart J Cardiovasc Imaging 2014;15:275-83.
16. Bateman TM, Berman DS, Heller GV, Brown KA, Cerqueira MD, Verani MS, et al. American Society of Nuclear Cardiology position statement on electrocardiographic gating of myocardial perfusion SPECT scintigrams. J Nucl Cardiol 1999;6:470-1.
17. Herzog BA, Buechel RR, Katz R, Brueckner M, Husmann L, Burger IA, et al. Nuclear myocardial perfusion imaging with a cadmium-zinc-telluride detector technique: Optimized protocol for scan time reduction. J Nucl Med 2010;51:46-51.
18. Cerqueira MD, Weissman NJ, Dilsizian V, Jacobs AK, Kaul S, Laskey WK, et al. Standardized myocardial segmentation and nomenclature for tomographic imaging of the heart. A statement for healthcare professionals from the Cardiac Imaging Committee of the Council on Clinical Cardiology of the American Heart Association. Circulation 2002;105:539-42.
19. Sharir T, Berman DS, Waechter PB, Areeda J, Kavanagh PB, Gerlach J, et al. Quantitative analysis of regional motion and thickening by gated myocardial perfusion SPECT: Normal heterogeneity and criteria for abnormality. J Nucl Med 2001;42:1630-8.
20. Germano G, Kavanagh PB, Waechter P, Areeda J, Van Kriekinge S, Sharir T, et al. A new algorithm for the quantitation of myocardial perfusion SPECT. I: Technical principles and reproducibility. J Nucl Med 2000;41:712-9.
21. Agostini D, Marie PY, Ben-Haim S, Rouzet F, Songy B, Giordano A, et al. Performance of cardiac cadmium-zinc-telluride gamma camera imaging in coronary artery disease: A review from the cardiovascular committee of the European Association of Nuclear Medicine (EANM). Eur J Nucl Med Mol Imaging 2016;43:2423-32.
22. Kacperski K, Erlandsson K, Ben-Haim S, Hutton BF. Iterative deconvolution of simultaneous 99mTc and 201Tl projection data measured on a CdZnTe-based cardiac SPECT scanner. Phys Med Biol 2011;56:1397-414.
23. Erlandsson K, Kacperski K, van Gramberg D, Hutton BF. Performance evaluation of D-SPECT: A novel SPECT system for nuclear cardiology. Phys Med Biol 2009;54:2635-49.
24. Ben-Haim S, Kacperski K, Hain S, Van Gramberg D, Hutton BF, Erlandsson K, et al. Simultaneous dual-radionuclide myocardial perfusion imaging with a solid-state dedicated cardiac camera. Eur J Nucl Med Mol Imaging 2010;37:1710-21.
25. Buechel RR, Herzog BA, Husmann L, Burger IA, Pazhenkottil AP, Treyer V, et al. Ultrafast nuclear myocardial perfusion imaging on a new gamma camera with semiconductor detector technique: First clinical validation. Eur J Nucl Med Mol Imaging 2010;37:773-8.
26. Mouden M, Timmer JR, Ottervanger JP, Reiffers S, Oostdijk AH, Knollema S, et al. Impact of a new ultrafast CZT SPECT camera for myocardial perfusion imaging: Fewer equivocal results and lower radiation dose. Eur J Nucl Med Mol Imaging 2012;39:1048-55.
27. Gimelli A, Bottai M, Giorgetti A, Genovesi D, Kusch A, Ripoli A, et al. Comparison between ultrafast and standard single-photon emission CT in patients with coronary artery disease: A pilot study. Circ Cardiovasc Imaging 2011;4:51-8.
28. Neill J, Prvulovich EM, Fish MB, Berman DS, Slomka PJ, Sharir T, et al. Initial multicentre experience of high-speed myocardial perfusion imaging: Comparison between high-speed and conventional single-photon emission computed tomography with angiographic validation. Eur J Nucl Med Mol Imaging 2013;40:1084-94.
29. Cochet H, Bullier E, Gerbaud E, Durieux M, Godbert Y, Lederlin M, et al. Absolute quantification of left ventricular global and regional function at nuclear MPI using ultrafast CZT SPECT: Initial validation vs cardiac MR. J Nucl Med 2013;54:556-63.
30. Jensen MM, Schmidt U, Huang C, Zerahn B. Gated tomographic radionuclide angiography using cadmium-zinc-telluride detector gamma camera; comparison to traditional gamma cameras. J Nucl Cardiol 2014;21:384-96.
31. Matsunari I, Saga T, Taki J, Akashi Y, Hirai J, Wakasugi T, et al. Improved myocardial fatty acid utilization after percutaneous transluminal coronary angioplasty. J Nucl Med 1995;36:1605-7.
32. Kawamoto M, Tamaki N, Yonekura Y, Tadamura E, Fujibayashi Y, Magata Y, et al. Combined study with I-123 fatty acid and thallium-201 to assess ischemic myocardium: Comparison with thallium redistribution and glucose metabolism. Ann Nucl Med 1994;8:47-54.
33. Taki J, Nakajima K, Matsunari I, Bunko H, Takata S, Kawasuji M, et al. Assessment of improvement of myocardial fatty acid uptake and function after revascularization using iodine-123-BMIPP. J Nucl Med 1997;38:1503-10.
34. Kawai Y, Tsukamoto E, Nozaki Y, Morita K, Sakurai M, Tamaki N. Significance of reduced uptake of iodinated fatty acid analogue for the evaluation of patients with acute chest pain. J Am Coll Cardiol 2001;38:1888-94.
35. Gibbons RJ, Chatterjee K, Daley J, Douglas JS, Fihn SD, Gardin JM, et al. ACC/AHA/ACP-ASIM guidelines for the management of patients with chronic stable angina: A report of the American College of Cardiology/American Heart Association Task Force on Practice Guidelines (Committee on Management of Patients With Chronic Stable Angina). J Am Coll Cardiol 1999;33:2092-197.
36. Iwado H, Iwado Y, Ohmori K, Mizushige K, Yukiiri K, Takagi Y, et al. Latent abnormal fatty acid metabolism in apparently normal perfusion during stress in patients with restenosis after coronary angioplasty: Assessment by exercise stress thallium-201 and iodine-123-labeled 15-(*p*-iodophenyl)-3-*R*, *S*-methylpentadecanoic acid-dual myocardial single-photon emission computed tomography. Am J Cardiol 2004;93:685-8.
37. Nakahara T, Hashimoto J, Suzuki T, Fujii H, Kubo A. Completely inverse images in dual-isotope SPECT with Tl-201 and I-123 MIBG in a patient with myocarditis. Ann Nucl Med 2001;15:277-80.
38. Ouyang J, Zhu X, Trott CM, El Fakhri G. Quantitative simultaneous 99mTc/123I cardiac SPECT using MC-JOSEM. Med Phys 2009;36:602-11.
39. Du Y, Tsui BM, Frey EC. Model-based crosstalk compensation for simultaneous 99mTc/123I dual-isotope brain SPECT imaging. Med Phys 2007;34:3530-43.
40. Blaire T, Bailliez A, Ben Bouallegue F, Bellevre D, Agostini D, Manrique A. First assessment of simultaneous dual isotope ((123)I/(99m)Tc) cardiac SPECT on two different CZT cameras: A phantom study. J Nucl Cardiol 2017;25:1692-704.
41. Kawai Y, Tsukamoto E, Nozaki Y, Kishino K, Kohya T, Tamaki N. Use of 123I-BMIPP single-photon emission tomography to estimate areas at risk following successful revascularization in patients with acute myocardial infarction. Eur J Nucl Med 1998;25:1390-5.